

Purdue University
Purdue e-Pubs

International Refrigeration and Air Conditioning
Conference

School of Mechanical Engineering

2016

Evaporation Heat Transfer and Pressure Drop of R32 inside Small-diameter 4.0 mm Tubes

Norihiro Inoue

Tokyo University of Marine Science and Technology, inoue@kaiyodai.ac.jp

Daisuke Jige

Tokyo University of Marine Science and Technology, djige00@kaiyodai.ac.jp

Kentaro Sagawa

Tokyo University of Marine Science and Technology, m154012@kaiyodai.ac.jp

Follow this and additional works at: <http://docs.lib.purdue.edu/iracc>

Inoue, Norihiro; Jige, Daisuke; and Sagawa, Kentaro, "Evaporation Heat Transfer and Pressure Drop of R32 inside Small-diameter 4.0 mm Tubes" (2016). *International Refrigeration and Air Conditioning Conference*. Paper 1730.
<http://docs.lib.purdue.edu/iracc/1730>

This document has been made available through Purdue e-Pubs, a service of the Purdue University Libraries. Please contact epubs@purdue.edu for additional information.

Complete proceedings may be acquired in print and on CD-ROM directly from the Ray W. Herrick Laboratories at <https://engineering.purdue.edu/Herrick/Events/orderlit.html>

Evaporation Heat Transfer and Pressure Drop of R32 inside Small-diameter 4.0 mm Tubes

Norihiro INOUE¹, Daisuke JIGE^{1*}, Kentaro SAGAWA²

¹ Tokyo University of Marine Science and Technology, Etchujima, Koto-ku, Tokyo, Japan
Phone number: +81-3-5245-7437, Fax number: +81-3-5245-7437,
E-mail address inoue@kaiyodai.ac.jp, djige00@kaiyodai.ac.jp

² Graduate School of Marine Science and Technology, Tokyo University of Marine Science and Technology, Etchujima, Koto-ku, Tokyo, Japan

ABSTRACT

This paper presents an experimental study of the pressure drop and evaporation heat transfer characteristics of R32 inside two horizontal small-diameter microfin tubes. The geometric parameters of the test microfin tubes are an outer diameter of 4.0 mm, 25 and 40 fins, helix angles of 16° and 17°, and fin heights of 0.1 and 0.2 mm. The pressure drop and evaporation heat transfer characteristics are measured in a mass velocity range of 50–400 kg/(m²s) and a heat flux range of 5–20 kW/m² at a saturation temperature of 15 °C. The pressure drop and evaporation heat transfer coefficient increase with increasing fin height and number of fins. The pressure drop and evaporation heat transfer characteristics in the small-diameter microfin tubes are also compared with those in a small-diameter smooth tube used as a reference tube. The pressure drop and evaporation heat transfer coefficient of the small-diameter microfin tubes are found to be, respectively, 1.1–2.0 and 1.3–6.5 times those of the small-diameter smooth tube having the same outer diameter.

1. INTRODUCTION

The recent development of high-performance, compact heat exchangers employing small-diameter tubes was necessitated by the need to improve the performance of heat exchangers and reduce the amount of refrigerant charge required for residential air-conditioning systems. It is necessary to clarify the pressure drop and heat transfer characteristics of boiling flow in order to facilitate the design of a heat exchanger. Conversely, in recent years, refrigerant R32—which has a lower global warming potential (GWP) than refrigerant R410A—has become commercially available for use in residential air-conditioning systems. A considerable amount of data on conventional large-diameter tubes is available; however, there is a scarcity of published data on the evaporation heat transfer and boiling flow characteristics of a small-diameter microfin tube.

Filho *et al.* (2004) performed experiments on the pressure drop of R134a boiling flow in horizontal smooth and microfin tubes in a mass velocity range of 70–1100 kg/(m²s). Further, Dang *et al.* (2010) investigated the evaporation heat transfer of CO₂ inside a small-diameter microfin tube with a mean inner diameter 2.0 mm in the mass velocity range of 360–720 kg/(m²s). Baba *et al.* (2012) experimentally investigated the pressure drop and heat transfer characteristics of R32 boiling flow and other refrigerants in a horizontal microfin tube with a mean inner diameter 5.2 mm. Wu *et al.* (2013) performed experiments of R22 and R410A inside a smooth tube and five microfin tubes with an outer diameter of 5 mm. Diani *et al.* (2014) performed experiments of R1234ze(E) inside small-diameter microfin tubes with a fin-tip diameter of 3.4 mm and outer diameter of 4 mm; they performed the experiments in a mass velocity range of 190–940 kg/(m²s) at a saturation temperature of 30 °C. They also proposed two prediction correlations for the heat transfer and pressure drop in microfin tubes. As mentioned above, only a few studies have been conducted on the evaporation heat transfer and pressure drop in microfin tubes with diameters smaller than 5 mm, particularly under low mass velocity and low heat flux conditions. In the present study, the evaporation heat transfer and pressure drop characteristics of R32 boiling flow in two horizontal microfin tubes with an outer diameter of 4.0 mm were investigated experimentally. The effects of microfin geometry on the evaporation

heat transfer and pressure drop characteristics were clarified. The evaporation heat transfer and pressure drop characteristics in the small-diameter microfin tubes were compared with those in a small-diameter smooth tube. The measured pressure drop was also compared with the values predicted using existing correlations.

2. EXPERIMENTAL APPARATUS AND METHOD

Figure 1 shows a schematic diagram of the experimental apparatus used in this study. The system consists of a magnetic gear pump, flow control valves, mass flow meter, water cooler, electric preheater, test section, condenser, liquid receiver, and subcooler. The liquid refrigerant discharged from the gear pump flows into the water cooler and electric preheater. The electric preheater heats the test refrigerant to achieve the desired vapor quality at the inlet of the test section. The liquid refrigerant returns to the gear pump through the condenser, liquid receiver, and subcooler. The refrigerant mass flow rate is measured using the Coriolis mass flow meter with an accuracy of $\pm 0.5\%$. The refrigerant flow rate is controlled mainly by the flow control valves of the main and bypass loops.

Figure 2 shows details of the test section. The test tube was directly heated by alternating current. The tube wall temperature was measured using T-type thermocouples with a measurement accuracy of ± 0.05 K. These thermocouples were inserted in the wall of the test tube at 50-mm intervals. The refrigerant pressures at the inlet of the measurement section were measured using an absolute pressure transducer with an accuracy of ± 1.4 kPa. The pressure drop between the inlet and outlet of the test section was measured using a differential pressure transducer with an accuracy of ± 0.2 kPa. The measurement lengths of heat transfer and pressure drop were 400 and 550 mm, respectively. The test section was enclosed in an insulator and placed in a temperature-regulated unit, where the temperature of the surrounding air was adjusted to the evaporation temperature of the test refrigerant at the test section in order to reduce heat gain from the surrounding air.

Table 1 presents the specifications of the test small-diameter smooth and microfin tubes. The outer diameter of both the small-diameter microfin tubes was 4.0 mm. Two small-diameter microfin tubes were tested in order to compare the effects of two different microfin geometries, i.e., the fin height and number of fins, on the evaporation heat transfer and pressure drop characteristics. The small-diameter smooth tube with the same outer diameter was also tested as a reference tube in order to investigate the effects of fins on the evaporation heat transfer and pressure drop characteristics, and the data obtained for this tube were considered as baseline data.

The experiments were performed using the test refrigerant R32 at a saturation temperature of 15 °C at the inlet of the test section. The mass velocity ranged from 50 to 400 kg/(m²s), and the heat flux ranged from 5 to 20 kW/m². The properties of the test refrigerant were calculated using NIST Refprop Ver.9.0 (Lemmon *et al.*, 2010).

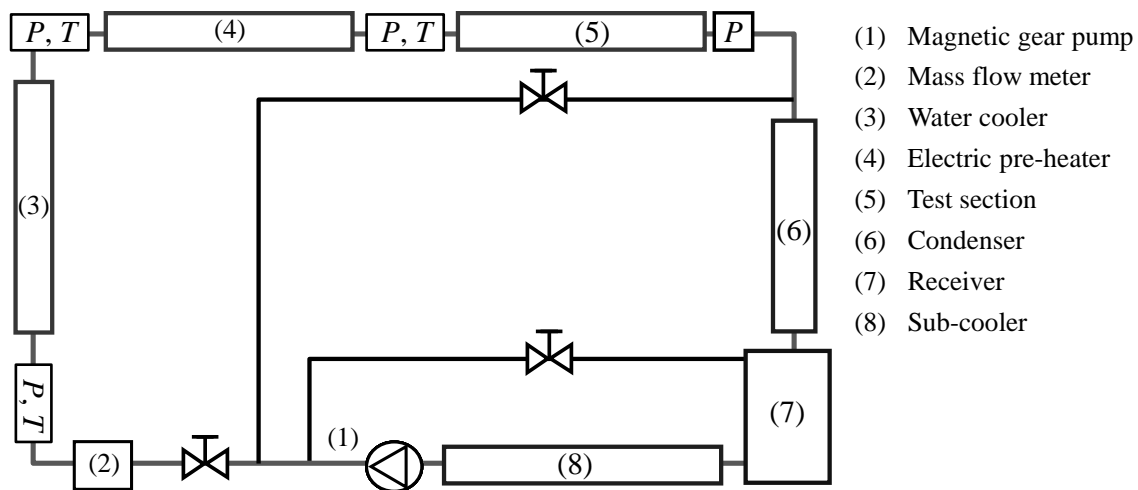


Figure 1: Schematic diagram of the experimental apparatus

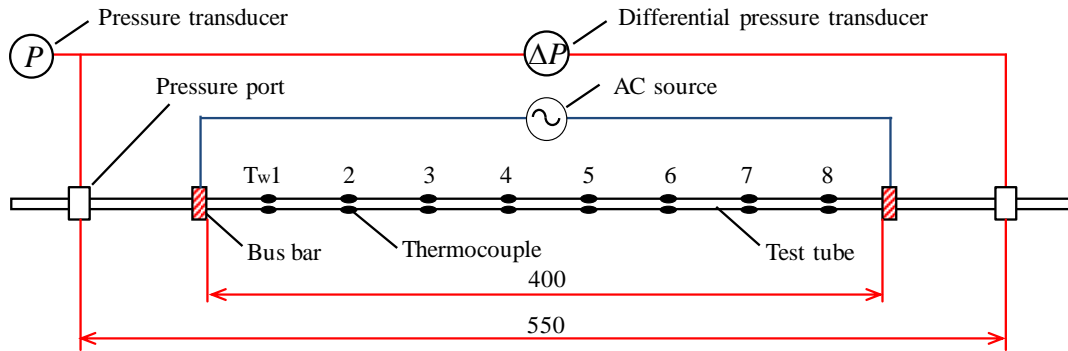


Figure 2: Detail of test section

Table 1: Specifications of small-diameter smooth and microfin tubes

Tube name	O.D. [mm]	Equivalent I.D. [mm]	Fin height [mm]	Number of fins [-]	Helix angle [°]
HF	4.0	3.5	0.2	40	17
LF	4.0	3.7	0.1	25	16
SM	4.0	3.5	-	-	-

3. DATA REDUCTION METHOD

The specific enthalpy at the inlet of the test section was calculated using the bulk specific enthalpy at the inlet of the electric preheater, the heat transfer rate, and the heat loss in the preheater. The bulk specific enthalpy at the inlet of the test section was calculated using the following heat balance equation:

$$h_{TS,in} = h_{E,in} + Q_E/m \quad (1)$$

where $h_{TS,in}$ and $h_{E,in}$ are, respectively, the bulk specific enthalpies at the inlets of the test section and the electric preheater; Q_E is the heat transfer rate in the electric preheater; and m is the flow rate of the test fluid. The distribution of vapor quality in the test section was determined using the bulk specific enthalpy calculated from the input heat transfer rate in the heating section. The heat flux q was calculated as follows:

$$q = Q_{TS}/A_H = Q_{TS}/(\pi \eta d_{eq} L) \quad (2)$$

where Q_{TS} is the heat transfer rate calculated from the inputted AC power in the heating section; and A_H , d_{eq} , and L are, respectively, the actual heat transfer area, equivalent inner diameter, and effective heating length of the test microfin tube. The evaporation heat transfer coefficient α is given by the following equation:

$$\alpha = q/(T_w - T_R) \quad (3)$$

where T_R is the refrigerant saturation temperature and T_w is the inner tube wall temperature. The tube wall temperature defined as the average of temperatures at the top and bottom of the test tube. The inner tube wall temperature was considered to be equal to the outer tube wall temperature.

For most of the obtained data, the uncertainty of the evaporation heat transfer coefficient was estimated to be within $\pm 10\%$, and the maximum error was evaluated to be up to 35% under the condition of a heat flux of 5 kW/m².

4. EXPERIMENTAL RESULTS AND DISCUSSION

4.1 Frictional Pressure Drop of Adiabatic Two-phase Flow

Figures 3(a) and 3(b) show the relationships between the frictional pressure drop gradient $\Delta P_F / \Delta Z$ and the vapor quality x of the adiabatic two-phase flow in the small-diameter smooth and microfin tubes at a saturation temperature of 15 °C and mass velocities of 100 and 400 kg/(m²s). The frictional pressure drops of the small-diameter smooth and microfin tubes were found to increase with increasing vapor quality and mass velocity. This is a consequence of the increasing vapor shear stress. The frictional pressure drop of the HF tube was 1.4–1.5 times that of the LF tube for the same vapor quality and mass velocity. This result is attributed to the flow loss due to an increase in the fin height and number of fins, particularly for low vapor velocities.

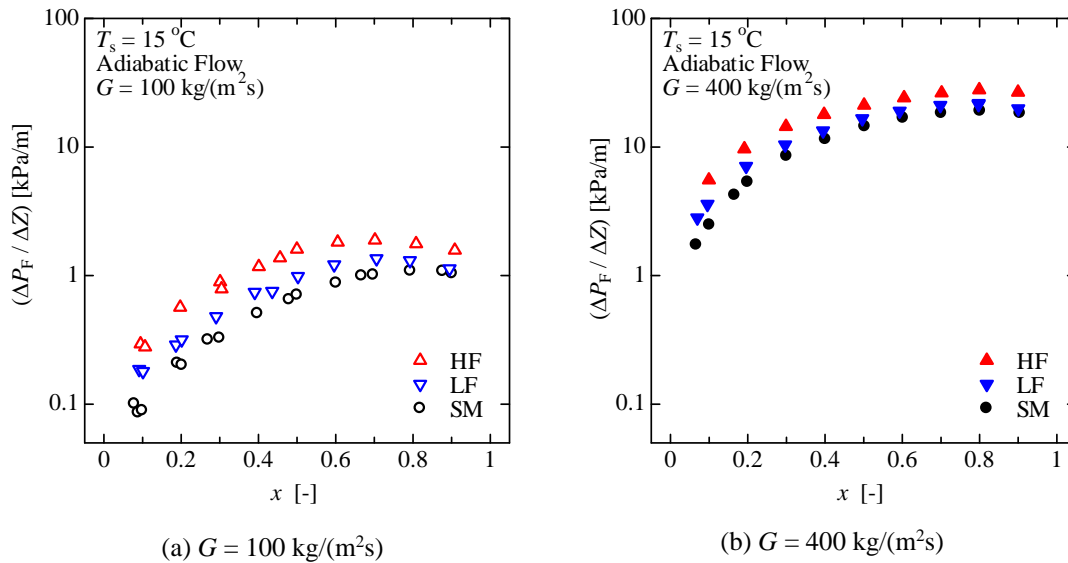


Figure 3: Pressure drops of R32 in small-diameter smooth and microfin tubes for adiabatic two-phase flow at a saturation temperature of 15 °C

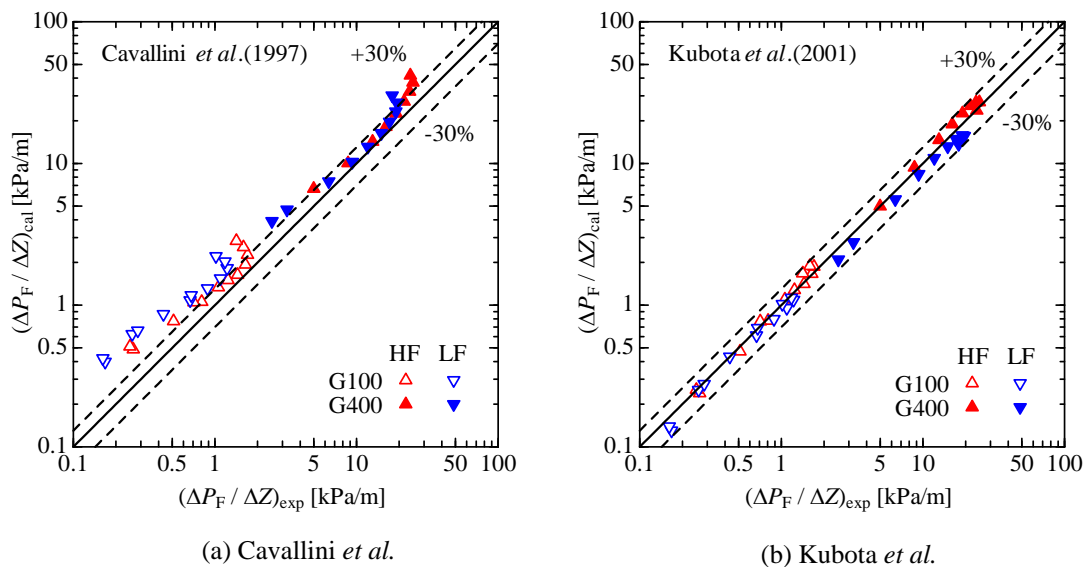


Figure 4: Comparison between measured and predicted frictional pressure drops

Figures 4(a) and 4(b) show a comparison between measured and predicted frictional pressure drops of the small-diameter microfin tubes (HF and LF tubes). The results obtained using the correlation of Cavallini *et al.* (1997) agree well with the present results for the mass velocity of 400 kg/(m²s), although this correlation overestimates the results for the mass velocity of 100 kg/(m²s). The results obtained using the correlation of Kubota *et al.* (2001) are in good agreement with the present results for both the mass velocities, i.e., 100 and 400 kg/(m²s).

4.2 Evaporation Heat Transfer Characteristics

Figures 5(a)–(d) show the measured heat transfer coefficients of the smooth and microfin tubes for mass velocities of 100 and 400 kg/(m²s) and heat evaporation fluxes of 5 and 20 kW/m² at a saturation temperature of 15 °C. Here, the horizontal and vertical axes represent the vapor quality x and the evaporation heat transfer coefficient α , respectively. Under both the heat flux conditions, at the mass velocity of 400 kg/(m²s), the evaporation heat transfer coefficient of the small-diameter smooth tube increases with increasing vapor quality, because the influence of forced convection becomes dominant. Forced convective heat transfer becomes the dominant heat transfer at high mass velocities and high vapor qualities. Conversely, nucleate boiling heat transfer becomes the dominant heat transfer at high heat fluxes and low vapor qualities.

The evaporation heat transfer coefficient of the small-diameter microfin tubes, i.e., the LF and HF tubes, is 1.3–6.5 times that of the small-diameter smooth tube under the same vapor quality, mass velocity, and heat flux conditions. The heat transfer characteristics, e.g., the forced convection and nucleate boiling heat transfer, of the small-diameter microfin tubes were observed, similarly to those of the small-diameter smooth tube, under the conditions of high mass velocity and heat flux. On the other hand, the evaporation heat transfer coefficients of the small-diameter microfin tubes are found to increase rapidly at the vapor quality of 0.4, mass velocity of 100 kg/(m²s), and heat flux of 5 kW/m² in comparison to that of the small-diameter smooth tube. The distribution of the measured tube wall temperature suggests that the flow pattern changes to separated flow with the thin liquid film at the top of the tube to enhance heat transfer by liquid surface tension and vapor shear stress. For further increase in vapor quality, the heat transfer coefficient rapidly decreases at over dryout vapor quality. With a further increase in the mass velocity, the liquid film covers the entire tube, including the fins. Therefore, the thin liquid film disappears as the film thickness becomes uniform.

Figures 6(a) and 6(b) show the relation between the measured heat transfer coefficients and the mass velocity for the small-diameter HF and LF tubes and that for the small-diameter smooth tube, respectively, at a vapor quality of 0.5 and a saturation temperature of 15 °C. In the figures, the horizontal and vertical axes represent the mass velocity G and the evaporation heat transfer coefficient α , respectively. At the heat flux of 5 kW/m², the evaporation heat transfer coefficient of the HF and LF tubes increases with increasing mass velocity in the range of 50–200 kg/(m²s). On the other hand, the evaporation heat transfer coefficient of the small-diameter smooth tube increases with increasing mass velocity because the influence of forced convection becomes dominant. However, the evaporation heat transfer coefficients of the HF and LF tubes at $G = 400$ kg/(m²s) are smaller than those at $G = 200$ kg/(m²s), despite the increase in the vapor shear stress. At the mass velocities of 100 and 200 kg/(m²s), the evaporation of the meniscus film in the fins improves with heat transfer; however, with a further increase in mass velocity, this film disappears owing to an increase in the vapor shear stress. At the heat flux of 20 kW/m², i.e., under a high heat flux condition, the evaporation heat transfer coefficient becomes constant, because the influence of nucleate boiling becomes dominant. The effect of fin geometry, i.e., the fin height and number of fins, is not observed at the mass velocity of 100 kg/(m²s) and heat flux of 5 kW/m². However, for $G > 100$ kg/(m²s) and at both the heat fluxes, i.e., 5 and 20 kW/m², the HF tube exhibits a larger evaporation heat transfer coefficient than the LF tube.

5. CONCLUSIONS

In this study, the evaporation heat transfer and pressure drop characteristics of R32 in horizontal small-diameter smooth and microfin tubes, where both these kinds of tubes had an outer diameter of 4.0 mm, were investigated experimentally. The main conclusions drawn from the experimental results are as summarized below.

- (1) The frictional pressure drop in the HF tube is 1.4–1.5 times that in the LF tube for the same vapor quality and mass velocity.
- (2) The predicted values obtained by the correlation of Kubota *et al.* (2001) agree relatively well with the values measured in the present study.

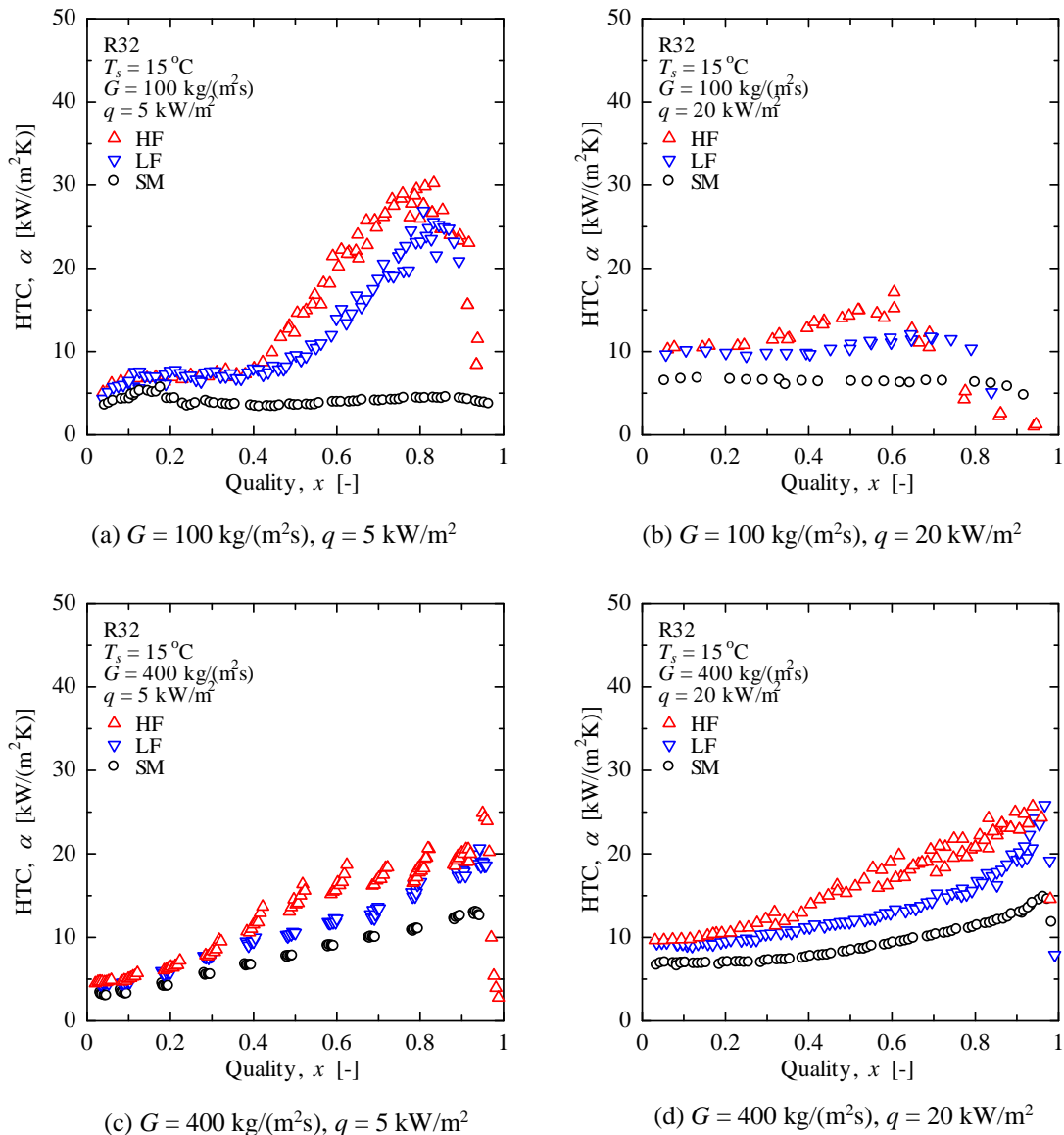


Figure 5: Heat transfer coefficient of R32 in small-diameter smooth and microfins tubes at saturation temperature of 15 °C

(3) Evaporation heat transfer characteristics, such as forced convection heat transfer, nucleate boiling heat transfer, and meniscus film evaporation heat transfer, are observed in the small-diameter microfins tubes. The evaporation heat transfer coefficients of the HF and LF tubes increase rapidly with increasing vapor quality owing to a change in the flow pattern to separated flow with the thin liquid film at the top of the tube to enhance heat transfer by surface tension and vapor shear stress.

(4) The evaporation heat transfer coefficient of the small-diameter microfins tubes, i.e., LF and HF tubes, is 1.3–6.5 times that of the small-diameter smooth tube under the same vapor quality, mass velocity, and heat flux conditions. The effects of fin geometry, i.e., fin height and number of fins, are not observed under low mass velocity and low heat flux conditions. However, at $G > 100 \text{ kg}/(\text{m}^2\text{s})$, regardless of the heat flux value, the HF tube exhibits a larger heat transfer coefficient than the LF tube.

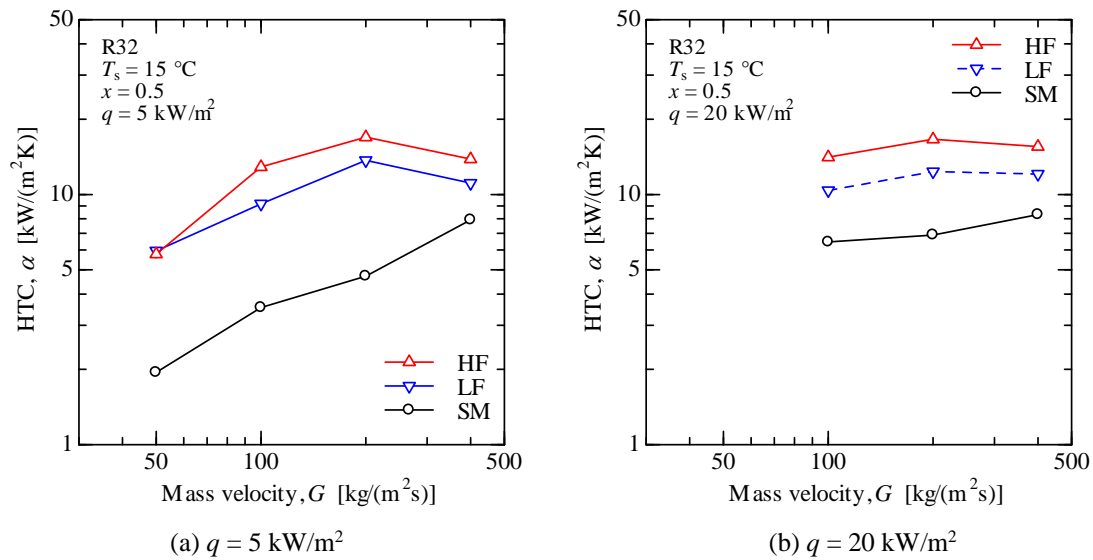


Figure 6: Heat transfer coefficient of R32 in small-diameter smooth and microfin tubes for vapor quality of 0.5 at saturation temperature of 15 °C

NOMENCLATURE

d	diameter	(m)
G	mass velocity	(kg/(m ² s))
h	specific enthalpy	(J/kg)
L	heat transfer length	(m)
Q	heat transfer rate	(W)
q	heat flux	(W/m ²)
T	temperature	(K)
T_s	saturation temperature	(K)
x	vapor quality	(-)
α	heat transfer coefficient	(W/(m ² K))
$\Delta P/\Delta Z$	pressure drop gradient	(Pa/m)
η	surface enlargement ratio	(-)

Subscripts

cal	calculation
E	electric preheater
eq	equivalent
exp	experiment
f	friction
in	inlet
R	refrigerant
S	smooth tube
ts	test section
w	tube wall

REFERENCES

- Baba D, Nakagawa T, Koyama S. 2012, Flow Boiling heat transfer and pressure drop of R1234ze(E) and R32 in a horizontal micro-fin tube, International Refrigeration and Air conditioning Conference, Paper 1218.
- Cavallini A, Del Col D, Doretti L, Longo GA, Rossetto L. 1997, Pressure drop during condensation and vaporization of refrigerants inside enhanced tubes, Heat and Technology. 15(1): 3-10.
- Dang C, Haraguchi N, Hihara E. 2010, Flow boiling heat transfer of carbon dioxide inside a small-sized microfin tube, Int. J. Refrig. 33: 655-663.
- Diani A, Mancin S, Rossetto L. 2014, R1234ze (E) flow boiling inside a 3.4 mm ID microfin tube, Int. J. Refrig. 47: 105–119.
- Filho EPB, Jabardo JMS, Barbieri PEL. 2004, Convective boiling pressure drop of refrigerant R-134a in horizontal smooth and microfin tubes, Int. J. Refrig. 27: 895–903.
- Lemmon EW, Huber ML, McLinden MO. 2010, Reference Fluid Thermodynamic and Transport Properties-REFPROP, Version 9.0, National Institute of Standards and Technology Standard Reference database, Gaithersburg.
- Kubota A, Uchida M, Shikazono N, 2001: Predicting Equations for Evaporation Pressure Drop Inside Horizontal Smooth and Grooved Tubes, Transactions of the Japan Society of Refrigerating and Air Conditioning Engineers. 18(4): 393-401. (in Japanese)
- Wu Z, Wu Y, Sunden B, Li W, Convective vaporization in micro-fin tubes of different geometries, Exp. Therm. Fluid Sci. 44 (2013) 398–408.

ACKNOWLEDGEMENT

This work was supported by the Japan Copper and Brass Association and Kobelco & Materials Copper Tube, Ltd. We would like to express our gratitude to both these organizations.